Application of Chemical Shift Imaging for Simultaneous and Fast Acquisition of NMR Spectra on Multiple Samples**

Alfred Ross,* Götz Schlotterbeck, Hans Senn, and Markus von Kienlin

NMR spectroscopy has become an indispensable part of molecular structure determination and verification processes in all fields of chemical and biostructural research. Only recently have the emerging field of combinatorial chemistry, in which large compound libraries need to be characterized, and the demand for quality control of compound depositories in pharmaceutical industry shown that the sample throughput achievable with setups used in modern NMR laboratories is too low and prevents efficient application of NMR spectroscopy in the above-mentioned contexts. The two automated setups nowadays in use comprise a) automated sample changers that position one NMR sample tube after the other in the magnet and b) the pumping of single samples in a capillary system to a properly designed flow-through probe.[1] Both approaches are designed for sequential sample input and lack any aspect of parallelization.

A setup with four detection volumes mounted into a home-built flow-through probe was described in the literature.[2] The application of an inhomogeneous magnetic z-field together with a tailored data processing was used to measure and decompose the spectra. This method, however, is restricted to measurements of only four samples in parallel and necessitates a coil around each sample tube. Therefore, a specially adapted NMR probe is needed.

To increase the parallelization and the sample throughput, as well as circumventing the need for additional costly hardware, we propose[3] the combination of a technique widely applied in the field of medical NMR spectroscopy known under the acronym CSI[4] (chemical shift imaging) with a compartmented detection volume realized by a bundle of 1-mm NMR-suited glass capillaries (Figure 1).[5] Each capillary is filled with a different solute. The acquisition of regular NMR data on such a compartmented detection volume results in a spectrum that is identical to that obtaind from a mixture of all the compounds in a single-volume detection cell. The decomposition of the data to single spectra is a prerequisite for getting useful information. We adopted the CSI technique that is in use in magnetic resonance imaging (MRI) to perform this task.[6] A typical question to be answered in medical applications of this technique is what is the spatial distribution of substances in certain organs within a human (animal) body. CSI combines spatial information (organs, for example, liver, or arbitrary coordinates) with chemical information (for example, the NMR spectrum of glucose).

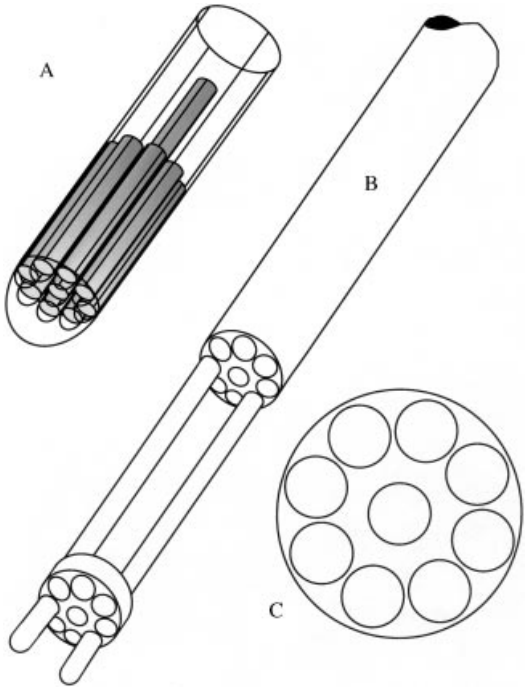

Figure 1. Schematic drawing (A and B) and cross section (C) of a nine-capillary bundle (A) to fit into a standard 5.0 mm NMR tube. The bundle is fixed at the bottom and the top in carriers made of plexiglas (B) in our in-house workshop. The upper carrier is integrated in a cylindrical module made of the same material to enable proper positioning in the NMR tube. To circumvent the need for cleaning the containers, disposable low-price capillaries can be used if a large number of samples have to be measured without significant loss of spectral quality.

The principle of the method rests on the application of controlled inhomogeneous magnetic field pulses (gradient pulses) to obtain information on the spatial distribution of spins within a sample volume.

Only recently were x- and y-direction gradient coils integrated in NMR spectrometers used in analytical chemistry for the purpose of coherence pathway selection and solvent suppression.[7] This hardware feature is commercially available for NMR spectrometers and meets exactly the requirements necessary to obtain spatially resolved chemical shift information. An exemplary pulse sequence suited for the acquisition of simple x,y-resolved one-dimensional (1D) ^{1}H NMR spectra is shown in Figure 2. The three-dimensional (3D) data set obtained comprises two spatial (x,y) dimensions and a spectral one. The initial phases of the free induction decays (FIDs) that were acquired as a function of the

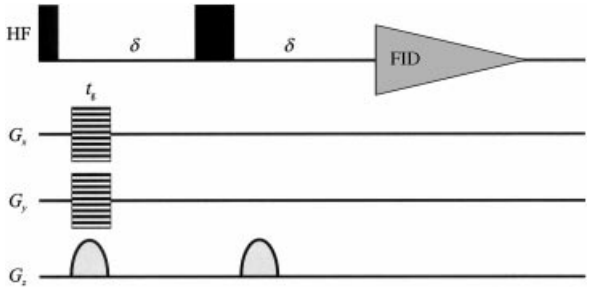

Figure 2. CSI pulse sequence for spatially x- and y-resolved 1D ^{1}H spectra.

[*] Dr. A. Ross, G. Schlotterbeck, H. Senn, M. von Kienlin
Pharma Preclinical Research Basel Technologies (PRBT-SR)
Hoffmann LaRoche AG
4070 Basel (Switzerland)
Fax: (+41)-61-688-7408
E-mail: alfred.ross@roche.com

[**] We gratefully acknowledge the competent support from H. J. Tschirky and his workshop.

  1433-7851/01/4017-3243 $ 17.50+.50/0

independently incremented gradient pulse strengths contains the information on the x and y position of the spins within the capillary bundle. The number of increments N_i and the strength G_i of the gradient pulses applied along a certain dimension $i \in \{x,y,z\}$ determine the so-called field-of-view (FOV_i), which is given by $2\pi(\gamma_H G_i t_g N_i)^{-1}$. The spatial resolution is given by FOV_i/N_i. All the FOV_i values must be set large enough to comprise the diameter of the object along the corresponding direction (for example, the diameter of the capillary bundle) to avoid folding. The spatial resolution must be set high enough to resolve the individual capillaries in the image. The parameters of the spectral dimension can be optimized as usual to enable extraction of chemical information as needed (chemical shift, J couplings, integrals). The spectral information is obtained as usual by Fourier transformation (FT) of the all FIDs with respect to the acquisition time. The image of the sample is obtained by independent FT of the data with respect to both incremented gradient strengths. It is clear from the theory of NMR imaging[8] that small "cross-talk" between extracted traces cannot be circumvented completely. Numerical simulation based on theory shows that the expected transfer of amplitudes between spectra in our experimental setup is below 6 % of the intensity of the spectrum of interest. This unwanted "contaminant" can be further reduced by use of optimized spatial sampling schemes.[9]

In Figure 3 we show the skyline projection of the data acquired as described in the Experimental Section after FT only with respect to the spatial dimensions. The expected

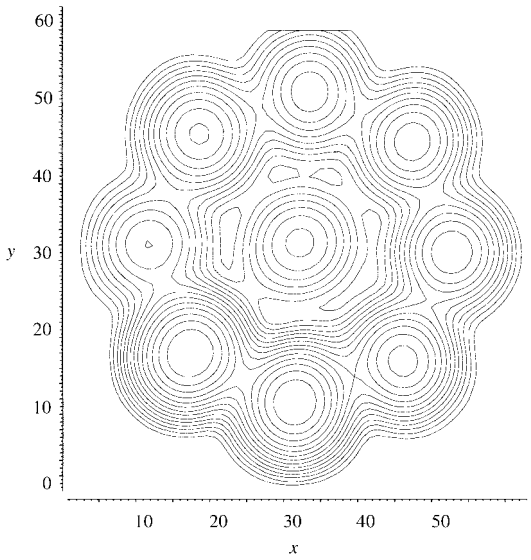

Figure 3. Cross-sectional image of the bundle of 1-mm capillaries obtained by FT along the spatial dimensions only. The contours code for spin density.

image of our object is clearly visible. The expanded regions of the spectra shown in Figure 4 were extracted after an additional FT with respect to the acquisition time, which was obtained from orthogonal traces taken out of the 3D data set at the x,y coordinates of the maxima located in each capillary. This task can be automated using known peak-picking algorithms. No cross-talk between the traces is seen at the given signal-to-noise level.

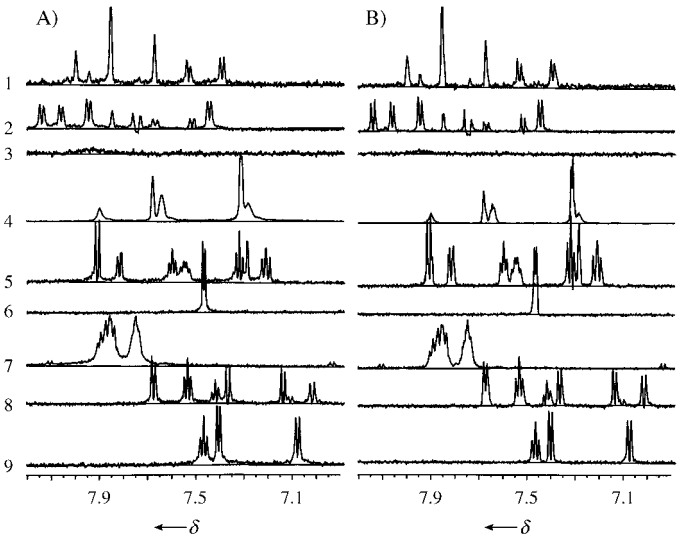

Figure 4. Expanded regions of the extracted ^{1}H 1D NMR spectra obtained with (A) and without (B) filling the interstice between the capillaries with [D_6]DMSO. The spectra allow for the extraction of chemical shifts and J couplings larger than 5 Hz. The reduced spectral resolution relative to those obtained from a standard setup can be explained by contributions to the B_0-field inhomogeneity from susceptibility jumps in our sample geometry. Nevertheless the quality of the spectra is high enough for structure validation of known structures needed for quality control of compound libraries. The signal-to-noise ratio measured fits (with the exception of the spectrum in trace 4) nicely with the expected value when taking into account the small detection volume per capillary. The result in trace 4 can be explained by a higher initial sample concentration. Trace 3 is blank as this substance has no aromatic moiety—signals are visible in other regions of this spectrum.

CSI is not restricted to the 1D homonuclear pulse sequence used here to extract chemical information. Multidimensional homo- and heteronuclear pulse sequences play a substantial role in modern NMR spectroscopy. The modification of most pulse sequences in use to include the spatial encoding part shown in Figure 2 prior to the detection of the signal is straightforward. As will be discussed below, a substantial decrease in the spectrometer time needed per sample by using the CSI technique is only achieved if the time needed for sample replacement dominates the total cycle time per sample in the conventional setup. This prerequisite can not be fulfilled by any multidimensional NMR experiment. The x,y-encoding scheme of an arbitrarily compartmented arrangement can easily be expanded by an additional incrementation of the strength of the z-gradient pulse to obtain spatial information along the z dimension of the compartment arrangement to obtain 3D spatial information.[10] This enables the application of the method to further optimized geometries of compartmentation.

The experimental time that allows a single scan per gradient setting is 5 min for our geometry of 9 samples. For comparison, an automated standard setup allows the acquisition of a simple 1D proton spectrum within 5.5 min per sample (typical cycle time in our service NMR department including automated sample exchange, shimming, locking). Thus, we have shown that an increase in the throughput of samples by a factor of roughly ten is readily achieved by use of CSI-based methods, and this can be performed on any commercially available state of the art NMR spectrometer. The only

  1433-7851/01/4017-3244 $ 17.50+.50/0

additional hardware needed is a miniaturized compartmented sample container suitable for NMR spectroscopy. For a typical small molecular weight substance, 30 μg dissolved in a capillary is enough to provide a spectrum of sufficient quality to deduce the structural integrity of the substance and impurities in the 10% range.

As the achievable signal-to-noise ratio is determined only by the sensitivity of the NMR probe and the number of spins in the detection volume, the method presented here by no means generates an improvement in the sensitivity of the NMR equipment. The gain in throughput is based solely on the reduction of the lengthy time required for frequent change of samples. This is only possible at the relatively high concentration of samples available in all fields mentioned in the introduction. Automation of the manually difficult filling of the capillary bundles is currently in progress in our workshop.[11] Further miniaturization of the diameters of the capillaries is due to limitations of available technology for automated liquid handling is not advisable.

The application of large diameter (7–10 mm) probes to increase the number of capillaries included in the detection volume is hampered by the lower intrinsic sensitivity of these probes, which reduces the quality of the spectra. This limitation might change in the near future if cryogenic technology[12] becomes available for larger diameter probes. A simple geometry for positioning 19 capillaries in a standard detection volume is described in the technical section. A bundle of flow-through capillaries measured by use of the CSI technique might also help to further increase the throughput of samples.

Experimental Section

For the experiments presented here each capillary tube was filled with 10 μL by using a syringe. The nine substances dissolved at concentrations below 10 mM in deuterated dimethyl sulfoxide ([D_6]DMSO) were arbitrarily obtained from our routine NMR laboratory. The solvent served as an internal lock. All data presented were taken on a DMX 600 Bruker spectrometer equipped with a standard triple-axis gradient TXI probe housing all the gradient coils. The temperature was set to 300 K. The NMR experimental parameters were set as follows: Proton pulse 8 μs; interscan delay 1 s; eddy current compensation δ 2 ms. FIDs of $4K$ complex time points were acquired in the digital filtering and quadrature detection mode of DMX spectrometers. The x- and y-gradient pulses ($t_g = 1$ ms) were ramped in 16 steps from -5 to $+5$ G cm^{-1} to obtain the needed spatial resolution of 300 μm. The 3 G cm^{-1} G_z gradient was used to remove 180° pulse imperfections.

This acquisition gave a data matrix of $(16 \times 16)_{\text{spatial}} \times 4K_{\text{complex,time}}$ data points. Eight dummy scans were allowed for thermal equilibration of the spin system prior to acquisition of the data. The data were processed using a matched exponential filtering along the chemical shift dimension and time-centered sine functions along both spatial dimensions together with first order phase correction (as needed) in all dimensions. Small truncation artifacts seen for multiplets are due to evolution of J-coupling during the spin-echo delays δ of the pulse sequence. A final data matrix of $(64 \times 64)_{\text{spatial}} \times 8K_{\text{chemical shift}}$ data points was obtained after zero filling. A bundle of capillaries (and interstice) filled with a 90% H_2O/D_2O mixture was used for a standard two-step z-gradient shimming protocol for the determination of initial shim settings. Low order off-axis shims were adjusted manually. The intercapillary space was originally filled with the same solvent as used in the capillaries to improve the homogeneity of the magnetic field over the bundle. Our highly symmetric arrangement comprises one central capillary surrounded by a second layer with eight capillary tubes. In the course of the experiments it turned out that the distortion of the magnetic field homogeneity introduced by the removal of the intercapillary liquid is negligible (Figure 4.). If the bundle is included in a standard NMR tube with a glass wall of 0.4 mm the active detection volume of the spectrometer cannot be filled completely with capillaries. The outer NMR tube is not necessary as the intercapillary liquid can be removed. Therefore, a bundle of 19 capillaries consisting of a central capillary surrounded by a second layer of 6 and a third layer of 12 capillaries will perfectly fill the available detection volume. Currently work is in progress in our laboratory to build such an improved geometry.

Received: May 10, 2001 [Z17073]

[1] M. Spraul, M. Hofmann, M. Ackermann, A. W. Nicholls, S. J. P. Damment, J. N. Haelden, J. P. Shockor, J. K. Nicholson, J. C. Lindon, *Anal. Commun*. **1997**, *34*, 339–341.

[2] E. MacNamara, T. Hou, G. Fisher, S. Williams, D. Raftery, *Anal. Chim. Acta* **1999**, *397*, 9–16.

[3] A. Ross, G. Schlotterbeck, H. Senn, *Eur. Pat. Appl.* 00810338.4, **2000**.

[4] a) A. Kumar, D. Welti, R. R. Ernst, *J. Magn. Reson*. **1975**, *18*, 69–83; b) T. R. Brown, B. M. Kincaid, K. Ugurbil, *Proc. Natl. Acad. Sci. USA* **1982**, *79*, 3523–3530; c) J. F. Martin, C. G. Wade, *J. Magn. Reson.* **1985**, *61*, 153–157; d) H. Rumpel, J. M. Pope, *Concepts Magn. Reson*. **1993**, *5*, 43–55.

[5] a) Wilmad Glass Buena, NJ 08310 (USA); b) Hilgenberg, 34323 Malsfeld (Germany).

[6] L. Brateman, *Am. J. Roentgenol.* **1986**, *146*, 971–980.

[7] T. Parella, *Magn. Reson. Chem*. **1998**, *36*, 467–495.

[8] a) F. J. Harris, *Proc. IEEE* **1978**, *66*, 51–55; b) M. von Kienlin, R. Pohmann in *Spatially Resolved Magnetic Resonance* (Eds.: P. Blümler, B. Blümich, R. Botto, E. Fukushima), VCH, Weinheim, **1998**, pp. 3–20.

[9] a) M. von Kienlin, R. Mejia, *J. Magn. Reson.* **1991**, *94*, 268–287; b) L. Bolinger, S. Leigh, *J. Magn. Reson.* **1988**, *80*, 162–167.

[10] A. A. Maudsley, S. K. Hilal, W. H. Perman, H. E. Simon, *J. Magn. Reson*. **1983**, *51*, 147–152; b) L. D. Hall, V. Rajanayagam, S. Sukumar, *J. Magn. Reson*. **1985**, *61*, 188–191.

[11] bai, 64686 Lautertal (Germany).

[12] P. J. Hajduk, T. Gerfin, J.-M. Boehlen, M. Häberli, D. Marek, S. W. Fesik, *J. Med. Chem.* **1999**, *42*, 2315–2317.

Landmark Crystal Structure of an Experimentally Utilized Tetralithium–Tetrapotassium Amide–Alkoxide Superbase**

Alan R. Kennedy, Jonathan G. MacLellan, and Robert E. Mulvey*

It has long been known that mixtures of organolithium derivatives (e.g., alkyls, amides, or enolates) and heavier alkali metal alkoxides (e.g. *tert*-butoxides or *tert*-pentoxides) can exhibit special proton-abstracting powers well beyond the capability of the lithium compounds on their own.[1] A forest of literature has grown around this superbasicity focussing mainly on its exploitation in organic synthesis[2] and, to a lesser extent in polymerization.[3] Yet for all this accumulated knowledge, there is still much uncertainty about the precise

[*] Prof. R. E. Mulvey, Dr. A. R. Kennedy, J. G. MacLellan
Department of Pure and Applied Chemistry
University of Strathclyde
Glasgow, G1 1XL (UK)
Fax: (+44) 141-552-0876
E-mail: r.e.mulvey@strath.ac.uk

[**] This work was supported by the UK Engineering and Physical Science Research Council.